

## Deformation phenomena in jointed rock\*

N. R. BARTON†

The role of rock joints in rock mass deformation phenomena is described. Individually, joints display concave-shaped stress–closure curves under normal loading and convex-shaped stress–displacement curves under shear, usually accompanied by dilation. The deformation behaviour of rock masses depends on the relative magnitudes of these components of closure, shear and dilation. The deformation of a rock mass may result in dramatic changes in the joint apertures and conductivities. Conversely, changes in joint water pressure cause changes in joint aperture which affect the overall deformation of the rock mass. Examples of compaction in jointed reservoirs and leakage phenomena in pressure tunnels are cited, each of which may be caused by changes in effective stress. The presence of rock joints is seen to affect stress slabbing phenomena in tunnels and is the suspected cause of depth-dependent contrasts of stress in sedimentary rocks. The phenomenon of hydraulic shearing of joints is discussed with particular reference to geothermal reservoir stimulation. Shearing is also the suspected mechanism in cases of mine flooding, following seismic loading. A method of modelling this dilation–conductivity coupling is presented. The Paper concludes by analysing the role of joint dilation in stress transformations and in the behaviour of underground openings. Rock masses have greater resistance to shear than predicted owing to non-coaxial stress and strain components. The shear strength and both the shear and normal stress components are affected by dilation.

L'article décrit le rôle joué par les joints des roches dans les phénomènes de déformation en masse des roches. Individuellement les joints montrent des courbes de contrainte–fermeture concaves sous des charges normales et des courbes de contrainte–déplacement convexes sous le cisaillement, généralement accompagnées de dilatance. Le comportement de déformation des masses rocheuses dépend des valeurs relatives de la fermeture, du cisaillement et de la dilatance. La déformation d'une masse rocheuse peut produire des changements dramatiques dans les ouvertures des joints et dans les conductibilités. Réciproquement, des changements dans la pression de l'eau dans les joints provoquent des changements dans leurs ouvertures qui affectent la déformation totale de la masse rocheuse. L'article mentionne des exemples de compactage dans des réservoirs jointoyés et des phénomènes de fuite dans des tunnels de pression. Chacun de ces exemples ayant pu être causé par des changements dans les contraintes effectives. On observe que la présence de joints dans les roches affecte les phénomènes de formation de dalles

par contrainte dans les tunnels et représente la cause présumée des contrastes de contrainte en profondeur dans les roches sédimentaires. On discute le phénomène du cisaillement hydraulique plus particulièrement eu égard à la stimulation géothermique des réservoirs. Le cisaillement est aussi la cause présumée de cas d'inondation de mines à la suite de chargements sismiques. Après avoir présenté une méthode pour modéliser cette combinaison de dilatance et de conductibilité l'article conclut par l'analyse de rôle joué par la dilatation des joints dans les transformations de contrainte et aussi dans le comportement des ouvertures souterraines. Les masses rocheuses ont une résistance au cisaillement supérieure à la valeur prédite, à cause des composantes non-coaxiales de déformation et de contrainte. La dilatance affecte à la fois la résistance au cisaillement et les composantes de cisaillement et de contrainte normale.

**KEYWORDS:** constitutive relations; deformation; pore pressures; rock mechanics; shear strength; tunnels.

### NOTATION

$d_n$	dilation angle
$e$	theoretical smooth wall conducting aperture of a joint
$E$	physical aperture of a joint
$e_0$	initial conducting aperture of a joint under nominally zero stress
$E_0$	initial physical aperture of a joint under nominally zero stress
$\Delta e$	change in conducting aperture
$\Delta E$	change in physical aperture
JCS	joint wall compression strength
JRC	joint roughness coefficient
$k$	joint conductivity, $e^2/12$
$L_n$	in situ block size (equal to the spacing of cross-joints)
$M$	deformation modulus
$\gamma$	density
$\delta$	shear displacement along a joint
$\delta_{\text{peak}}$	shear displacement at peak shear strength
$\sigma_h$	minor or intermediate horizontal principal stress
$\sigma_H$	major horizontal principal stress
$\sigma_n$	normal stress
$\sigma_v$	vertical principal stress
$\tau$	shear stress
$\phi_b$	basic friction angle (unweathered rock surface)
$\phi_p$	peak friction angle

\* 8th Laurits Bjerrum Memorial Lecture.

† Norwegian Geotechnical Institute, Oslo.

$\phi_r$  residual friction angle (weathered rock surface)

*Subscript*

mob mobilized at any instant, e.g.  $JRC_{mob}$ ,  $d_{nmob}$

INTRODUCTION

Rock joints play three fundamental roles in the behaviour of rock masses. Each are closely coupled. Briefly stated rock joints provide most of the weakness, deformability and conductivity of typical rock masses. One talks of the shear strength of joints but worries more about their potential weakness. Values of stiffness are estimated when really softness is meant, since joints have a much lower stiffness than the intact rock.

The parameters strength and stiffness are strongly stress dependent and may vanish under tensile stress. When under compression, however, they vary between fairly well understood limits. The parameter which varies most of all under varying compression and shear is the joint aperture. Quadratic and cubic relationships between aperture, conductivity and flow rate cause dramatic coupling between the hydraulic and mechanical behaviour.

The complex deformation phenomena observed in jointed rock masses can be more readily understood when the individual components of deformation are separated. In most competent rock masses, the intact material separating the joints can be considered as elastic or pseudoelastic. Relative to the joints, intact rock is generally stiff, and its high modulus is complemented by a low value of Poisson's ratio. Lateral expansion is limited, at least at moderate stress levels.

The second component of deformation is the normal stress-closure behaviour of the joints. Fig. 1 shows that, when the deformation of the intact rock ( $\Delta V_r$ ) is subtracted from the stress-closure curve for the whole jointed block ( $\Delta V_j$ ), a highly non-linear, hysteretic stress-closure curve is obtained for the individual joint ( $\Delta V_i$ ).

The first cycle of loading shown in Fig. 1 displays larger hysteresis than subsequent cycles due to sample disturbance effects. However, some hysteresis and marked non-linearity are typical characteristics of rock joints under normal loading, even after many cycles of loading and unloading.

The third and potentially largest component of deformation of a rock mass is the joint shear component. The marked convex shape of shear stress-displacement curves contrasts strongly with the concave shape of stress-closure curves. Fig. 2 indicates that a marked sample size effect

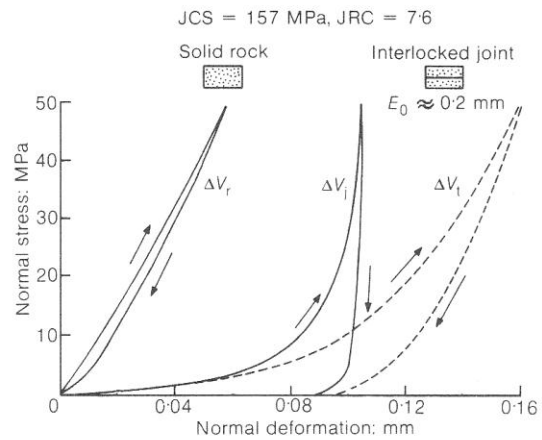


Fig. 1. Concave normal stress-deformation behaviour of rock joints (after Bandis, Lumsden & Barton, 1983) ( $\Delta V_r$  is the deformation of the rock and joint,  $\Delta V_r$  is the deformation of the rock alone and  $\Delta V_j$  is the net deformation of the joint)

may also be present, if the joints are non-planar. Both the peak shear strength and the displacement required to reach peak strength are affected by sample size.

Papers by Barton & Choubey (1977), Bandis *et al.* (1981), Barton & Bandis (1982) and Bandis *et al.* (1983) describe how these components of deformation and scale effects can be predicted, using the simple index test methods illustrated in Fig. 3.

Figure 3(a) illustrates self-weight tilt tests performed on blocks of natural size. Large diameter core samples can also be used, as illustrated by the four cored holes. When smaller samples are used (Fig. 3(b)) scale corrections are applied,

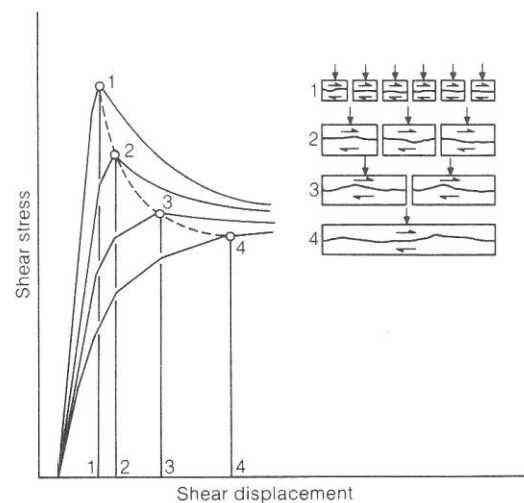


Fig. 2. Convex shear stress-displacement behaviour of rock joints, illustrating sample size dependence (after Bandis, Lumsden & Barton, 1981)

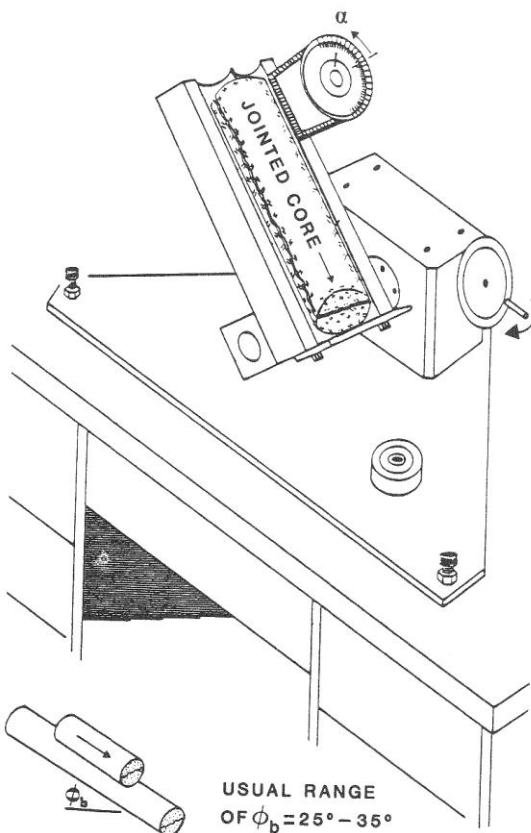
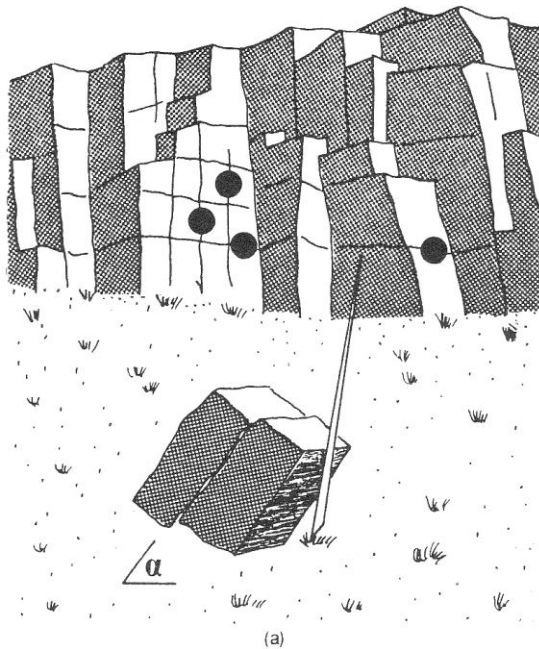


Fig. 3. Tilt tests for obtaining joint roughness and basic friction parameters

since small samples display larger tilt angles than naturally jointed blocks. Tilt tests on core sticks (Fig. 3(b), inset) provide estimates of the basic friction angle  $\phi_b$  of smooth unweathered rock surfaces.

An additional test not shown in Fig. 3 is the Schmidt hammer rebound test, which is used to measure the compressive strength of the joint wall material. The index parameters required for complete joint characterization can be defined as follows

JRC	joint roughness coefficient
JCS	joint wall compression strength
$\phi_r$	residual friction angle
$e$	theoretical conducting aperture
$E$	physical joint aperture

The last two parameters are utilized when coupling joint deformation with conductivity, as described by Barton, Bandis & Bakhtar (1985).

#### DEFORMATION MODES FOR ROCK MASSES

Information on rock mass deformation moduli is required in the design of arch dams and bridge piers, and in all tunnelling projects where analysis of deformations is required. The most realistic data are obtained from large-scale tests in which the jointing is fully represented. On many occasions, owing to the prevalence of horizontally bedded sedimentary rock, the load-deformation curves obtained from large plate loading tests resemble the normal closure curves for rock joints, as depicted in Fig. 1.

Such curves can be characterized as type A behaviour, as shown schematically in Fig. 4. In general, joints parallel to the bedding are subjected to normal closure. Lateral expansion is limited, and shear components are largely absent.

Renewed interest in the deformability of rock masses has been evident in a number of large-scale tests funded under nuclear waste storage programmes. Cramer, Cunningham & Kim (1984) describe large-scale *in situ* block tests performed at the Near Surface Test Facility at the Hanford Site, USA, on columnar basalt. An initially surprising result from these tests was the comparative linearity of the load-deformation curves when loading was perpendicular to the basalt columns. The usual concave behaviour was absent during loading but was evident during unloading. Type B behaviour illustrated in Fig. 4 suggests that a combination of shearing and normal closure may be occurring. The linear behaviour found by Cramer *et al.* (1984) presumably results from the superposition of concave (closure) and convex (shear) components.

Large-scale *in situ* biaxial tests of jointed gneiss reported by Hardin, Barton, Lingle, Board &

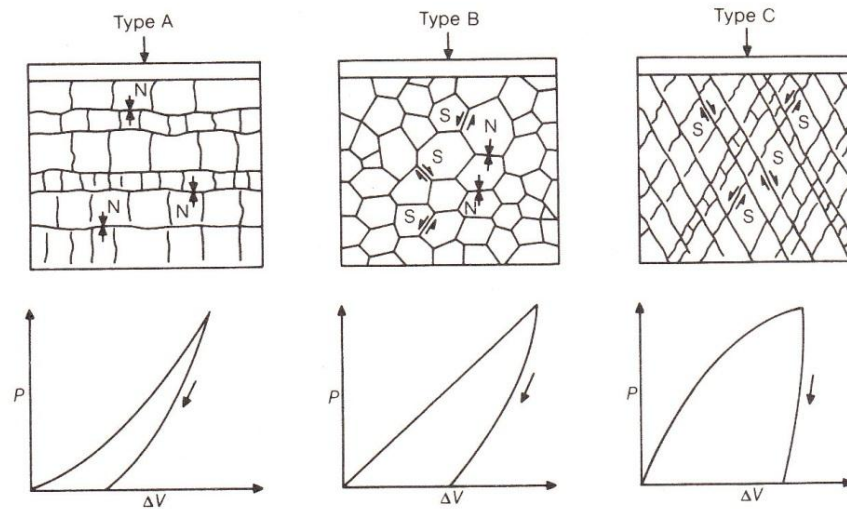


Fig. 4. Contrasting load-deformation ( $P$ - $\Delta V$ ) behaviour for rock masses with different magnitudes of joint shear (S) and normal deformation (N) components

Voegele (1982) were specially designed so that major joints could be loaded in shear. The major joints formed diagonals across the cubic block of rock, which was loaded on four vertical sides using flatjacks. The measured behaviour resembled type C in Fig. 4, with distinctly convex load-deformation behaviour and marked hysteresis.

These behaviour modes are summarized in Table 1.

An additional factor that affects the deformation mode is the block size and/or number of blocks tested. Barton & Bandis (1982) found that a fundamental change in behaviour occurs when a very large number of blocks are loaded. Model tests on type C assemblages using biaxial shear loading showed convex, i.e. normal, behaviour when loading 250 and 1000 block models.

However, when the number of blocks was increased to 4000, the axial load-deformation curves were distinctly linear. In each of these type C models, the ratio of lateral to axial strain increased with mobilization of shear from 0 through 1.0 to approximately 2.0, when major shear failures occurred.

The familiar concept of Poisson's ratio for an elastic solid is clearly inapplicable to a shearing,

dilating assemblage of blocks, especially, when deformations are large.

#### EFFECT OF JOINTING ON STRESS SLABBING

The relatively low strength and deformable nature of rock joints frequently causes problems in rock engineering. However, one particular aspect of joint behaviour may be positive in the special case of excavation in highly stressed rock masses.

Dynamic release of thin plates of rock from tunnel walls (stress slabbing) may occur in an underground excavation if too much extensional strain is experienced by the rock in question. The seriousness of occurrence is dependent on rock type since it has been shown by Stacey (1981) that intact rock tolerates extensional strain to varying degrees. However, if jointing is present, extensional strain and shear strain can be accommodated readily. Paradoxically, the excavation of an underground opening in a highly stressed environment is likely to be less hazardous when the rock is jointed than when it is intact.

This hypothesis may be thoroughly tested when a nuclear waste repository is finally con-

Table 1. Three characteristic load-deformation behaviours for rock masses

Type	Dominant mode	Shape	Hysteresis	Lateral expansion
A	Normal	Concave	Small	Small
B	Normal and shear	Linear	Moderate	Moderate
C	Shear	Convex	Large	Large

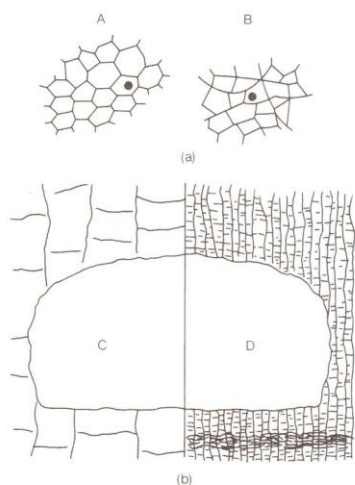


Fig. 5. Large relative block sizes experienced by boreholes A and B cause borehole wall failure ('dog-eared')—tunnels driven in the same highly stressed rock might suffer stress slabbing in case C but not in case D, owing to the strain relieving nature of the joints: (a) boreholes in 'massive' rock; (b) tunnels in jointed rock

structed in the Hanford basalts in Washington State, USA. Virgin stress levels in the candidate basalt Cohasset flow are as follows (Long, 1983)

$$\sigma_H = 52.5\text{--}63.4 \text{ MPa (major horizontal component)}$$

$$\sigma_h = 30.3\text{--}35.6 \text{ MPa (minor horizontal component)}$$

$$\sigma_v = 23.1\text{--}23.2 \text{ MPa (vertical component)}$$

The high levels of differential stress ( $\sigma_H/\sigma_v = 2.3\text{--}2.7$ ) cause extensive core discing in the relevant 900–1000 m depth, and borehole walls are extensively damaged ('dog eared'), with increased dimensions across their E–W diameters, perpendicular to the  $\sigma_H$  direction. It has been estimated that, when thermal loading is superimposed on the virgin stress field, due to the highly radioactive waste, the effective value of  $\sigma_H$  may be as high as 100 MPa locally, resulting in stress concentrations as high as 150 MPa round the planned elliptically shaped waste emplacement tunnels.

Application of the tunnel reinforcement guidelines in the Q system (Barton, 1984) to this problem suggests that mild rock bursting or stress slabbing will occur in the massive colon-

nade section of the basalt flow, with its characteristic hexagonal columns, but is unlikely in the more heavily jointed entablature. The occurrence of 'dog-earing' in excavations of borehole size may well be due to the relative scarcity of strain relieving joints at this scale. As suggested in Fig. 5, the problem is dependent on relative block size which can be defined as the ratio of the excavation span and the average block size.

Physical model studies reported by Barton & Hansteen (1979) provide some support for this hypothesis. Model tunnels were excavated in highly anisotropic stress fields. In most of the excavations, the smallest top headings had a relative block size of 1/12, i.e. 12 blocks per span width. In no cases were blocks fractured by the highly anisotropic stress. Tunnel deformation was marked (0.5% of span) and was caused mainly by extensional strain relief and shear on the joints.

A model with particularly large joint spacing was specially constructed to facilitate simulation, using a jointed finite element code. The model contained only 1200 discrete blocks instead of the usual 20000 blocks. It had the same extreme stress distribution, the same joint orientations and the same excavation methods were used. Deformation around the opening was greatly reduced, and stress slabbing was observed when the relative block size was 1/2. Clearly jointing can be advantageous when excavating in high stress fields.

#### EFFECTS OF JOINTING ON STRESS CONTRASTS

As shown in Fig. 1, rock joints display hysteretic, non-linear behaviour when normal stresses are cycled. This characteristic shape of the stress-closure curves may be the reason for reversal of stress magnitudes measured during small volume hydraulic fracturing (minifrac) stress measurements at different depths.

Deep oil and gas reservoirs generally have higher minimum principal stress levels in barrier shales than in reservoir sandstones. A typical unpublished result is shown in Fig. 6.

Stress measurements at much shallower depth reported by Barton (1983) apparently show the opposite of the behaviour at depth. These shallower measurements were performed in interbedded shales, siltstones and sandstones at 100–200 m depth. The minimum levels of horizontal stress were measured in the shales, and the highest in the sandstones. (These results are shown later in another context.) In both the cases referred to, the stresses were measured by the minifrac (hydraulic fracturing) technique.

Figure 7 illustrates schematically the relatively

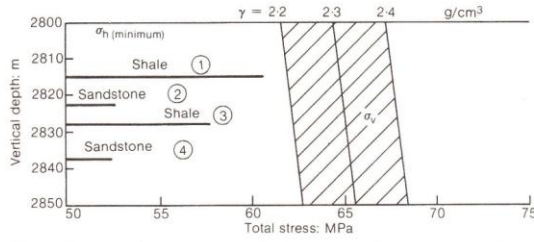


Fig. 6. Contrasts in minimum principal stress typically seen in deep oil and gas reservoirs: these contrasts are apparently reversed at shallow depth

linear elastic load–deformation behaviour of a hypothetical intact sandstone reservoir rock. The figure also illustrates a more hysteretic stress–closure curve for a hypothetical fissile shale. If it is assumed that stress measurements made under continental land masses involve rocks that are on the erosional (unloading) side of one of their stress cycles, then the unloading moduli  $M_1$  and  $M_2$  (deep burial) and  $M_3$  and  $M_4$  (shallow burial) will be the relevant stiffnesses for interpreting behaviour.

In this hypothetical example,  $M_2$  (shale) is greater than  $M_1$  (sandstone) at great depth, while at shallow depth  $M_4$  (shale) is less than  $M_3$  (sandstone). It is well known that in layered elastic materials high modulus layers attract the highest stresses and low modulus layers the lowest stresses. This could explain the reversal of

the minimum stress levels in shale and sandstone seen in measurements at depth and near the surface.

JOINT APERTURE AND CONDUCTIVITY PHENOMENA

The distribution of joint apertures in a rock mass is a feature that can be changed dramatically by human intervention. Deformation strains as small as fractions of a per cent in the rock mass as a whole may result in major changes in joint apertures. These in turn can have dramatic effects on the joint conductivity, on leakage rates and on the ease of grouting. Before investigating the magnitude of potential aperture changes, it is necessary to consider the size of undisturbed apertures and their related conductivity.

Several methods of estimating initial joint aperture have been discussed in recent articles in the rock mechanics literature. These range from direct optical measurement across thin-sectioned epoxy-grouted joints, statistical or empirical treatment of joint surface roughness, to indirect measurement using closely spaced straddle packers in borehole pumping tests. Tests by indirect measurement reported by Davison, Keys & Paillet (1982) indicated a lognormal distribution of theoretical smooth wall conducting apertures over the depth range 7–475 m, with a median value of 25  $\mu\text{m}$ .

A statistical interpretation of borehole pumping tests using constant packer spacing can also be used to obtain estimates of conducting aperture, as described by Snow (1968). Numerous tests performed at US dam sites in the depth range 0–60 m indicated that conducting apertures were mostly in the range 50–150  $\mu\text{m}$  at this shallow depth.

Interest in joint apertures has been particularly stimulated by the current international nuclear waste disposal studies. These have emphasized the need to interpret joint apertures in at least

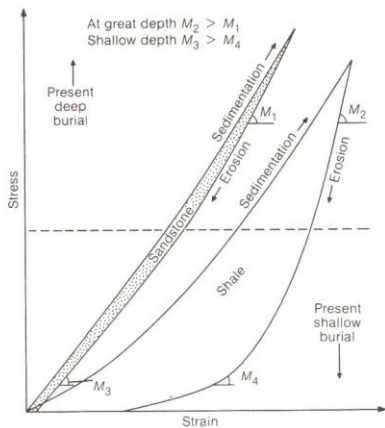


Fig. 7. Possible explanation for the reversal in stress contrasts seen in deep and shallow sediments due to deformation modulus changes (after Barton, 1983)

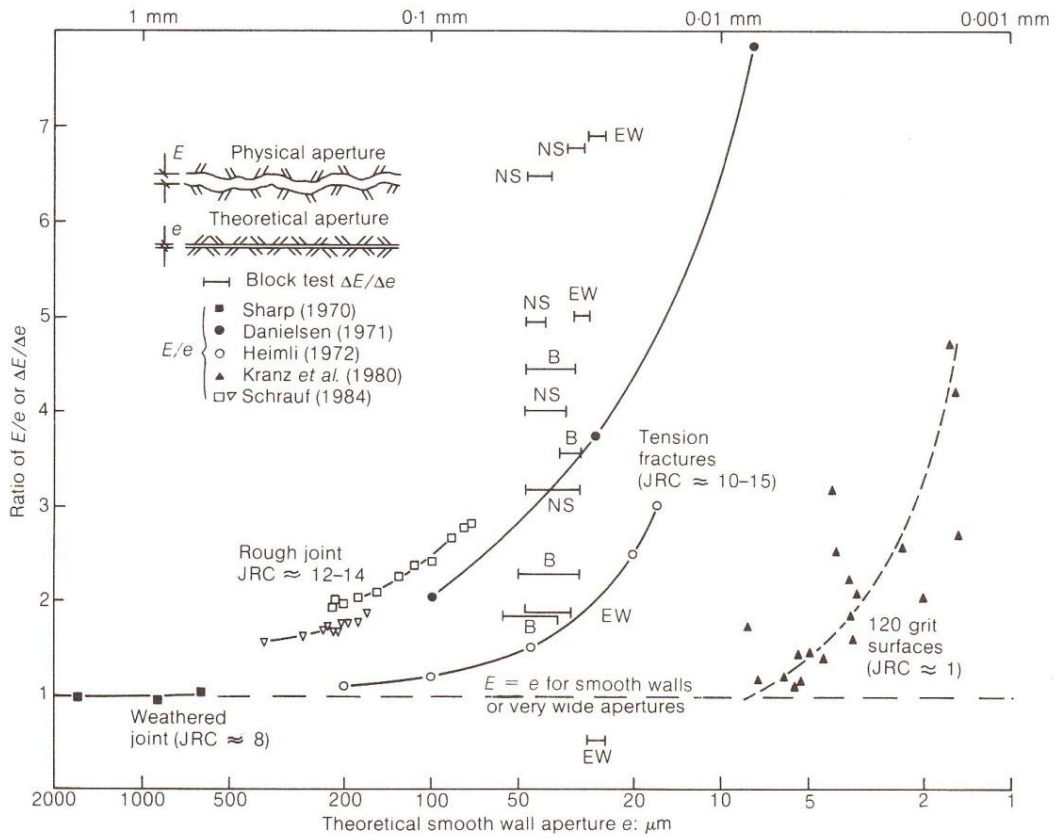


Fig. 8. Comparison of real physical apertures  $E$  with theoretical smooth wall conducting apertures  $e$ : the mismatch is caused by flow losses due to contacting areas, channelling and surface roughness (after Barton *et al.*, 1985)

two ways. Stress change, caused by excavation or thermal loading, results in a change in the physical aperture ( $\Delta E$ ), but this may be of different magnitude to the corresponding change in conducting aperture ( $\Delta e$ ).

The physical aperture  $E$  and the theoretical smooth wall conducting aperture  $e$  are of unequal magnitude, as shown by the experimental data presented in Fig. 8. The discrepancy is due to the frictional drag of rough joint walls, and the tortuous flow path in the plane of the joint caused by areas of contact. These effects increase at higher stress levels.

These factors need to be taken into account when converting stress-closure behaviour to stress-conductivity behaviour, where conductivity  $k$  is given by

$$k = e^2/12 \quad (1)$$

The data presented in Fig. 8 can be approximated by an empirical equation incorporating a suitable term for roughness. A convenient term is the joint roughness coefficient JRC obtained from the simple tilt tests illustrated in Fig. 3.

*Estimation of grout-take for jointed rock*

The volume of a rock mass that can be grouted is related to the porosity of the joint network and is therefore represented more closely by the physical aperture  $E$  than by the conducting aperture  $e$  of the joints. When  $e$  is interpreted from borehole pumping tests using Snow's (1968) statistical method, the median value obtained needs to be converted to  $E$  using the data presented in Fig. 8.

Figure 9 illustrates the assumed cubic network of conducting apertures which is the Snow (1968) idealization of a permeable, jointed rock mass. These theoretical conducting apertures  $e$  have been converted to physical (real, rough-walled) apertures  $E$  using data from Fig. 8.

This method of porosity and grout-take estimation takes into account the channelling of flow known to occur in the plane of each joint due to contacting areas. However, the data base represented in Fig. 8 is incomplete. Furthermore, the method does not allow for the different degrees of joint deformation that occur when flow testing with water with linear or logarithmic pressure decay or for the more uniform pressure distribu-

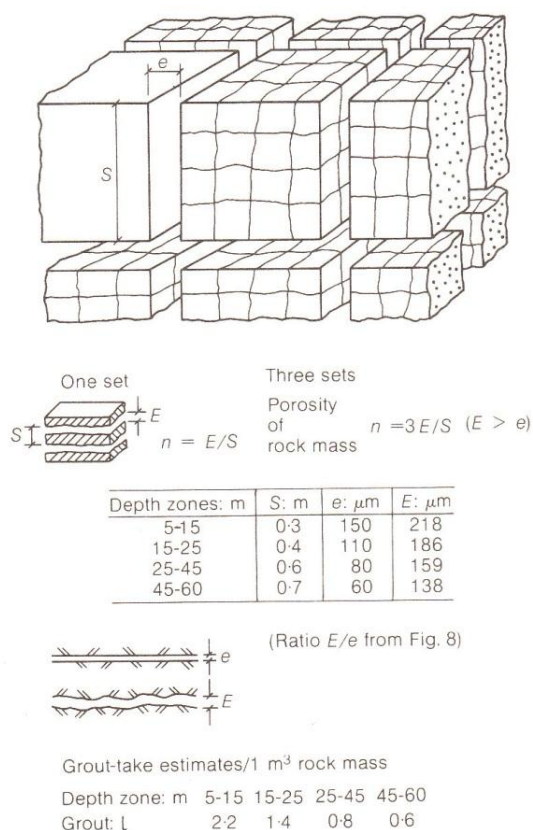


Fig. 9. Example of grout-take estimation by converting theoretical conducting apertures  $e$  obtained from water injection tests to physical apertures  $E$  using experimental data from Fig. 8 (assumed cubic network of water conducting joints based on Snow (1968))

tion that is built up across a joint plane when grout is beginning to stiffen. The latter may jack open the more conductive joints to a greater extent than occurs under a water flow test. Grout-take estimates can therefore be underestimated.

#### COMPACTION AND DEPLETION PHENOMENA IN JOINTED RESERVOIRS

The stress-closure behaviour of individual joints illustrated in Fig. 1 has now been mathematically modelled using a hyperbolic function (Bandis *et al.*, 1983)

$$\frac{\Delta V_j}{\sigma_n} = a - b \Delta V_j \quad (2)$$

where  $\Delta V_j$  is the joint closure,  $\sigma_n$  is the effective normal stress and  $a$  and  $b$  are abscissae. The maximum joint closure  $V_m$  is equal to  $a/b$ , and the initial normal stiffness  $K_{ni}$  is equal to  $1/a$ .

Estimates of  $V_m$  and  $K_{ni}$  for successive loading and unloading cycles are given by Bandis *et al.*

(1983) and are based on the index parameters JRC (joint roughness coefficient), JCS (joint wall compression strength) and  $E_0$  (initial joint aperture under zero stress).

A numerical model and plotting routine described by Barton & Bakhtar (1983a) allow stress-closure behaviour to be predicted over four cycles of loading, given appropriate input data (JRC, JCS,  $E_0$ ) and the desired range of effective normal stress.

Figure 10(a) illustrates a typical set of stress-closure curves, with input data measured from jointed core, as depicted in Fig. 3. Values of conducting aperture  $e$  and physical aperture  $E$  are labelled at the three stress levels shown. In Fig. 10(b) the stress-closure behaviour has been extended to stress-conductivity coupling, using equation (1) and data from Fig. 8.

It is instructive to consider a hypothetical well drawdown (depletion) history. Suppose that an over-pressured, jointed reservoir suffers a gradual 15 MPa reduction in reservoir pressure. Initial conditions might be

Total rock stress 30 MPa  
Reservoir pressure 25 MPa

The effective normal stress is therefore increased from 5 MPa to 20 MPa during the 15 MPa pressure depletion. The numerical model shown in Fig. 10 predicts individual joint closures of 21.3  $\mu\text{m}$  and a 50% reduction in conductivity (from  $3.2 \times 10^{-6} \text{ cm}^2$  to  $1.5 \times 10^{-6} \text{ cm}^2$  or from 320 to 150 darcies) as a result of this depletion process. This would have dire economic consequences for the jointed reservoir in question.

Cumulative closures on thousands of flat lying joints or shear on numerous steeply dipping joints could also alter the total compaction and subsequent subsidence experienced above a large jointed reservoir. Sea bed subsidence above a large North Sea chalk reservoir is currently causing concern owing to small margins of platform 'daylight' above the maximum wave heights. Wave heights that are larger than originally expected in combination with a subsidence of several metres cause increased moments on production platforms. It is therefore important to predict subsidence magnitudes with greater accuracy than may be required above land-based reservoirs.

#### LEAKAGE PHENOMENA IN PRESSURE TUNNELS

Pressure tunnels for conventional and pumped hydro projects are frequently concrete lined. Efforts are usually made to estimate or measure the deformation modulus of the surrounding rock

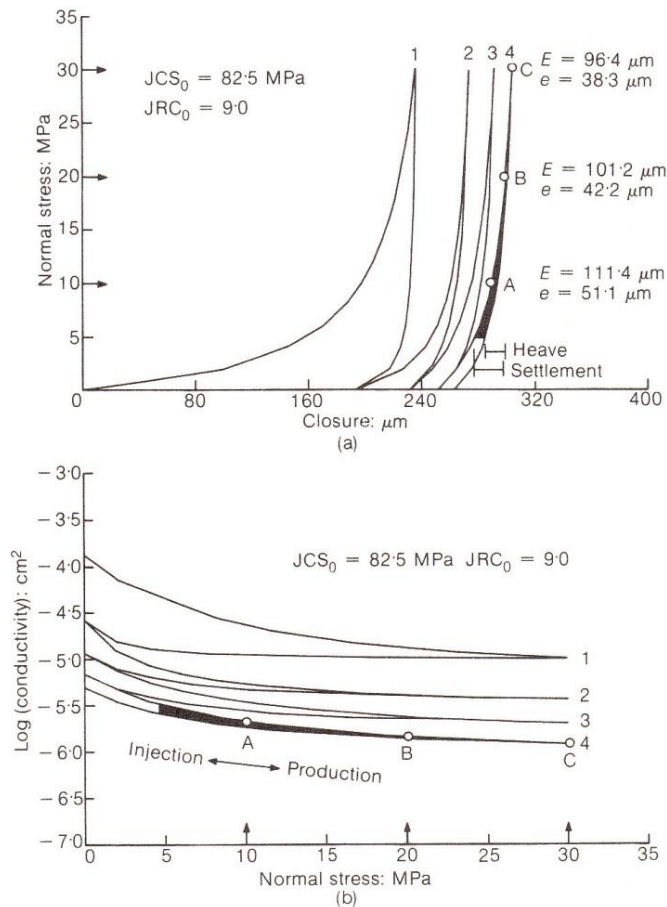


**Fig. 10. Coupled stress-closure-conductivity model which provides important input to the compaction and depletion modelling of jointed reservoirs**

so that load sharing can be designed. However, it is not infrequently that heavy steel reinforcement needs to be used to assist the concrete-rock interaction in resisting the water load. This measure is taken when the rock is of low modulus, and also when the depth to overburden is inadequate. The steel reinforcement is designed to distribute any cracking that might occur around the periphery, so that cracks are very fine and result in marked head losses. The likelihood and consequences of hydraulic splitting (or joint opening) in the surrounding rock mass is thereby reduced.

The length of reinforced concrete required is often based on overburden calculations. The maximum water pressure is compared with the minimum rock stress. Stress calculations are modified to allow for sloping valley sides, and a safety factor is chosen to take care of dynamic water pressures. However, stress measurements, for example using the minifrac (hydraulic fracturing) technique, may demonstrate that

minimum horizontal stresses are lower than the assumed vertical gravitational stress. Fig. 11 shows six measured values of  $K_0$  ( $\sigma_h/\sigma_v$ , total stresses) in the range 0.44–0.52 for interbeds of shale. These low values resulted in an expensive extension of the steel reinforcement.

A water pressure less than the minimum principal stress would appear to remove the threat of hydraulic fracturing of the rock mass. However, an especially interesting leakage phenomenon has been observed in several pressure tunnels in Norway and elsewhere. The locations of these leakages are usually immediately upstream of the concrete plug separating the unlined section of the pressure tunnel from the steel-lined section.

Leakages have occurred even when conventional overburden design criteria are satisfied with large factors of safety.

It has been suggested by Andersen (1970) that increased effective normal stress causing joint closure downstream of the plug is a plausible

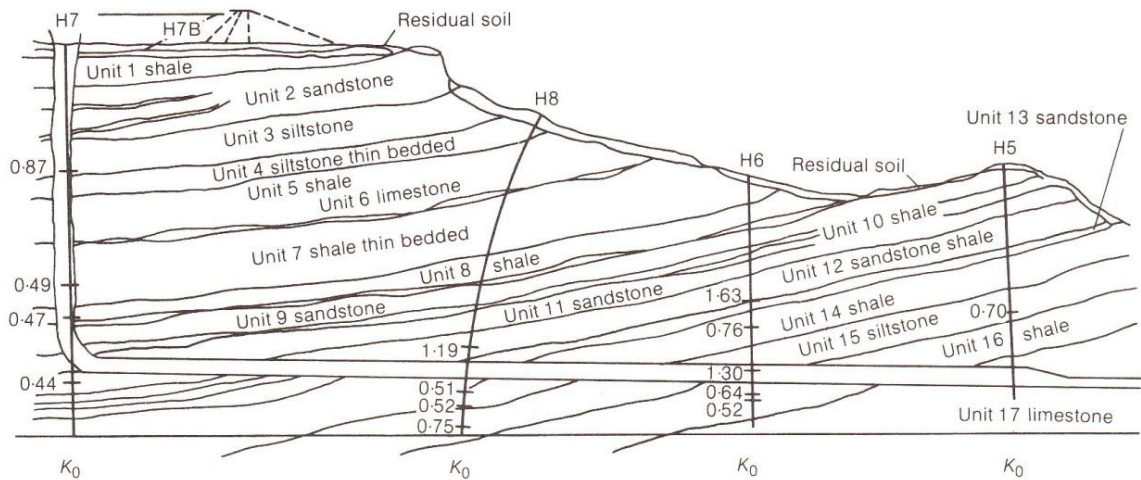


Fig. 11. Minifrac stress measurements showing low values of  $K_0$  ( $=\sigma_h/\sigma_v$ ) in interbeds of shale above a pressure tunnel (after Barton, 1983)

mechanism for the development of these leakages. Fig. 12 illustrates schematically the process that may be involved. Before construction of the pressure tunnel the rock joints are under a certain level of effective normal stress. Construction will cause some local groundwater drawdown, but it is reasonable to expect that the groundwater level will be re-established, perhaps exceeded, when the unlined section of the pressure tunnel is under full head.

Downstream of the plug, if the steel liner is not cast in concrete and contact grouted, there will be an open annulus around the liner that is under atmospheric pressure. Drainage towards this

annulus, as illustrated in Fig. 12, will result in increased effective normal stress and consolidation (joint closure) in this zone, all the way around the tunnel.

This consolidation mechanism will probably cause extension in the zone immediately upstream of the plug where the effective normal stress is already lower. Any possible shearing mechanism due to unfavourable jointing might further facilitate such a transfer of strain in the rock mass. On occasions joints have opened several centimetres with leakage all the way to the valley side, in addition to leakage around the plug (Lien & Valstad, 1971). Conditions are worsened if the vertical joints depicted in Fig. 12 are filled with deformable material that can also be washed out of the joints, such as silt or sand.

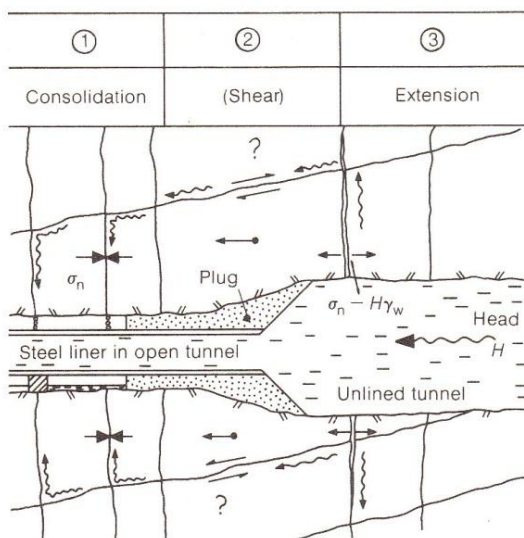


Fig. 12. Potential leakage mechanism around a concrete plug separating an unlined pressure tunnel from the steel-lined section

HYDRAULIC SHEARING PHENOMENA

Enormous sums of money are spent each year in attempting to fracture tight reservoir formations hydraulically, to increase conductivity towards the wells. The success rate is moderate, and there have been notable failures. Risks are minimized, though not removed, by conducting minifrac stress measurements to determine contrasts in minimum stress as illustrated in Fig. 6. If bottom hole treatment pressures are limited to the minimum total stress measured in the barrier rock, there is a reasonable chance that a massive hydraulic fracture (MHF) will be contained more or less within the reservoir rock or pay zone.

The theory of minifrac stress measurement and MHF treatments is based on the assumption that the fracture will leave the well in the two positions round the circumference where the original compressive stresses are a minimum. In intact

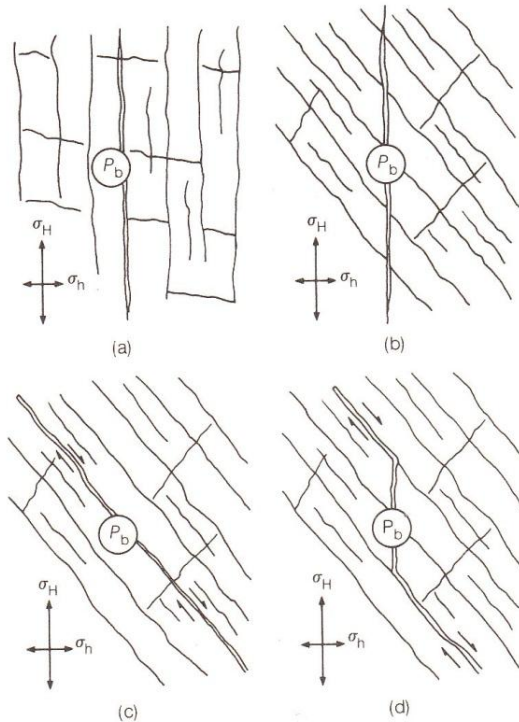


Fig. 13. Illustrations of (a) hydraulic jacking, (b) hydraulic fracturing and (c) hydraulic shearing: (d) shows the combined mode (the breakdown pressure  $P_b$  will be different for cases (a), (b) and (c))

rock, these locations will be the first where extensional strains are registered during pressurization. Once developed, the fractures will continue to propagate parallel to the major principal stress and perpendicular to the minor principal stress. In cased wells, the fracture will propagate from a perforation, and bend into the theoretical plane with continued pumping if it initiates in the wrong location.

When stress measurements or MHF treatments are performed in fractured (jointed) petroleum reservoirs, such as sandstone, limestone, chert or chalk, the interpretation of the stress measurements and the success of the MHF treatment is less certain. Several variations in behaviour can be considered. If dominant subvertical jointing parallels the principal horizontal stress, hydraulic fracturing will tend to jack open the existing joints or at least run parallel to them, as illustrated in Fig. 13(a).

If, in contrast, the major jointing is inclined to the principal stress, quite different behaviour may occur. First consider that the joints are extremely tight and high bottom hole pressures are used. The scenario depicted in Fig. 13(b) may then occur, at least in the immediate vicinity of the well. However, if the major jointing is more per-

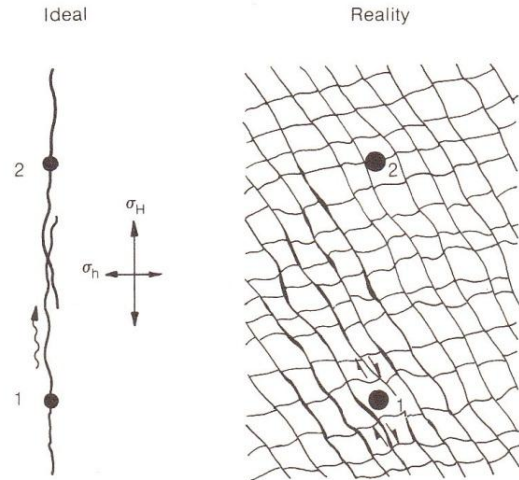


Fig. 14. Schematic diagram of the hydraulic shearing phenomenon experienced in some geothermal projects: pumping into hole 1 causes joint shearing instead of the intended hydraulic fracturing

meable and pumping capacity is limited, it is likely that the obliquely oriented joints will be activated in preference to fresh fracturing. In this case hydraulic jacking will be replaced by hydraulic shearing if horizontal stress contrasts exist. The scenario depicted in Fig. 13(c) (or combined mode Fig. 13(d)) will result in shear displacements, dilation and massive increases in conductivity parallel to the major joints.

Current hydrothermal projects run by Los Alamos National Laboratory in the USA (Murphy, Kepler & Dash, 1983) and by Camborne School of Mines in Cornwall (Pine & Batchelor, 1984) have apparently encountered hydraulic shearing mechanisms in their attempts to develop hydraulic fractures between wells. In these projects fracturing is designed to obtain larger surface areas for heat exchange and to obtain improved connection between wells (Fig. 14).

In the Cornwall project two wells were drilled to a depth of 2 km and aligned relatively to each other so that they would be approximately parallel to  $N 50^\circ W$ , the direction of the major horizontal stress. At this depth  $\sigma_H$  and  $\sigma_h$  had values of 70 MPa and 30 MPa in total stress terms. Pine & Batchelor (1984) reported that approximately 300 000  $m^3$  of water had been injected into the granitic rock mass, using downhole pressures in excess of 30 MPa.

Numerous microseismic events were detected during pumping, and hydraulic shearing was presumed to be migrating downwards, perhaps due to the fundamental curvature of the peak shear strength envelope for rock joints as stress is increased. The major set of subvertical joints

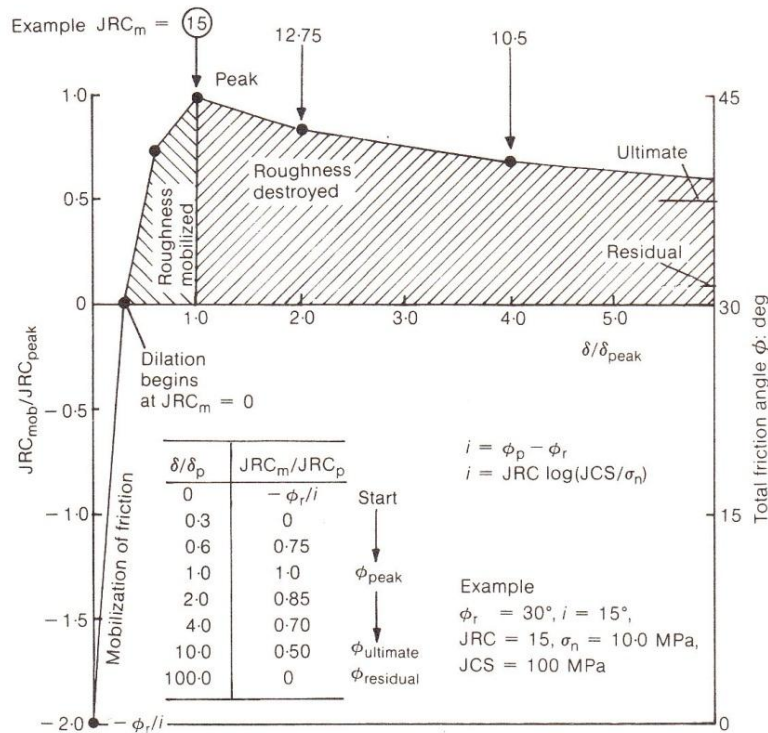


Fig. 15. Dimensionless model for shear stress–displacement modelling (after Barton, 1982): in this example  $\phi_r/i = 2$

identified as the source of shearing strike at  $30^\circ$  from the major horizontal stress.

During pumping into one well the pressure was observed to fall in the adjacent well due presumably to the periodic dilation of the surrounding rock mass. Pine & Cundall (1985) have modelled this hydraulic shearing mechanism using a modified version of the distinct element finite difference code (UDEC) developed by Cundall (1980). A suitable joint constitutive model that takes into account variable roughness, wall strength and block size is obviously important to obtain the critical relationship between shear displacement and dilation, and associated coupling with conductivity. One such model is described in the next section.

MODELLING SHEAR, DILATION AND CONDUCTIVITY COUPLING

The shear stress–shear displacement curves illustrated in Fig. 2 indicate that block size has an important effect on shear strength and shear stiffness, particularly in the initial phases of shearing. The radial change in the shape and slope of the curves as block size changes cannot be readily modelled by a mathematical function, as was the case for normal closure (equation (2) and Fig. 10).

The approach that has been developed is illustrated in Fig. 15. The shear strength mobilized

$\phi'_{mob}$  at any given displacement  $\delta$  can be expressed by the following general equation

$$\phi'_{mob} = JRC_{mob} \log(JCS/\sigma'_n) + \phi_r \quad (3)$$

where  $JRC_{mob}$  is the mobilized roughness and  $\sigma'_n$  is the effective normal stress.

The following key aspects of behaviour are modelled in the order in which they occur during a shearing event.

- (a) Friction is mobilized when shearing begins.
- (b) Dilation begins when roughness is mobilized.
- (c) Peak shear strength is reached at  $JRC_{mob}/JRC_{peak} = 1.0, \delta/\delta_{peak} = 1.0$ .
- (d) Dilation declines as roughness reduces.
- (e) Residual strength is finally reached.

Dilation modelling is based on an empirical equation that is closely related to equation (3)

$$d_n\text{ mob} = \frac{1}{2}JRC_{mob} \log\left(\frac{JCS}{\sigma'_n}\right) \quad (4)$$

In both equations (3) and (4) the value of  $JRC_{mob}$  refers to the full-scale roughness, which is smaller than the roughness measured on smaller samples. For example, when referring to the tilt tests shown in Fig. 3, the test on the natural block would be considered to give full-scale values of

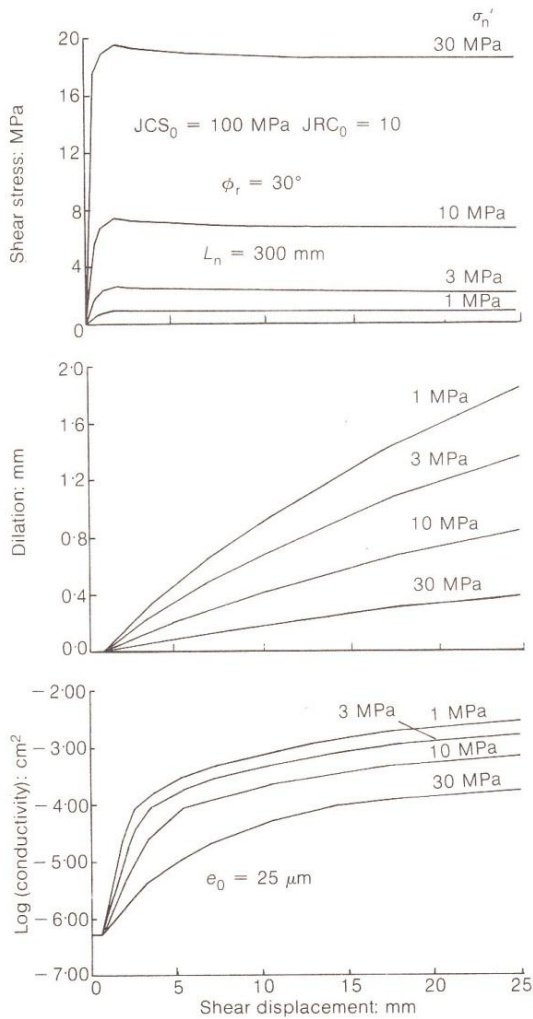


Fig. 16. Effect of normal stress variation on the coupled behaviour of joints, when an average block size of 300 mm is assumed

JRC, while the tilt tests on the smaller (and shorter) jointed core would give artificially high values. Methods of scaling the values of JRC and JCS obtained from small-scale tests are described by Barton *et al.* (1985).

An important component of the hydraulic shearing phenomenon described earlier is the coupling of conductivity with dilation. A certain initial aperture  $E$  is increased by the process of dilation as follows

$$\Delta E = \Delta \delta \tan d_{n\text{mob}} \quad (5)$$

where  $\Delta E$  is the increment in aperture and  $\Delta \delta$  is the increment in shear displacement.

Values of  $E + \Delta E$ , which are physical apertures, are converted to theoretical smooth wall conducting apertures  $e$  using an empirical equation derived from the experimental data presented

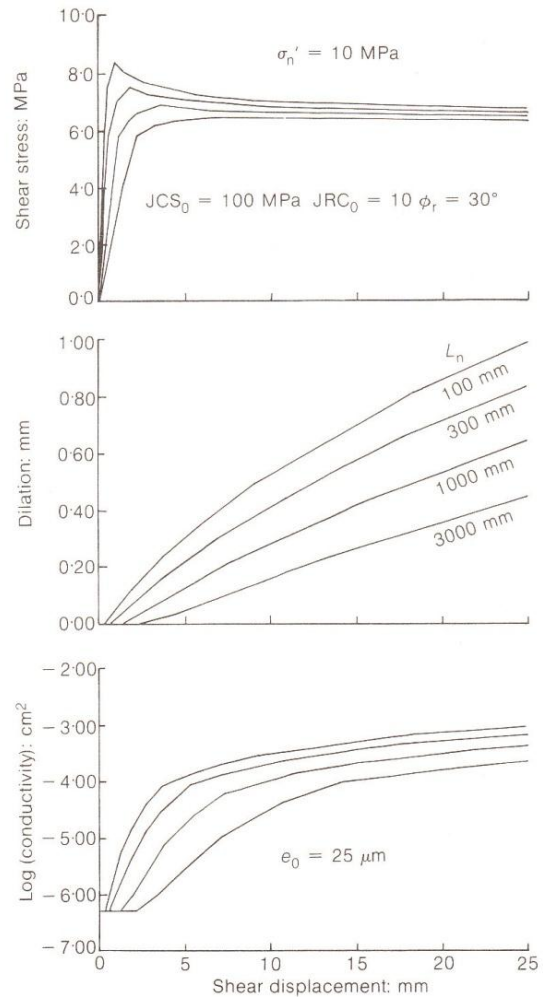


Fig. 17. Effect of variations in sample size on coupled behaviour, assuming a constant effective normal stress of 10 MPa

in Fig. 8. The resulting conductivities are obtained from equation (1).

Example plots showing coupled behaviour are given in Figs 16 and 17. It will be noticed that a range of block sizes  $L_n$  from 100 mm to 3000 mm produces nearly as large a range of dilation and conductivities as a range of effective stress from 1 MPa to 30 MPa. However, stress variation affects shear strength to a greater extent than block size. The range of results illustrated makes it easy to see why hydraulic shearing can cause problems in trying to establish good hydraulic connection in a reservoir.

Coupled flow-displacement shear tests on joints, currently being conducted at the Norwegian Geotechnical Institute by Makurat (1985), indicate similar magnitudes of coupling to those predicted here. Tests on a natural joint in gneiss

of 150 mm length have demonstrated an at least two orders of magnitude increase in conductivity in the first millimetre of shear. Effective normal stress levels were difficult to hold constant during shear but were generally in the range 1–3 MPa.

#### COUPLED PHENOMENA DURING SEISMIC LOADING

A number of references to mine flooding or increased flows of water as a result of earthquakes are given in the literature. There are also occasional references to greatly diminished flows. Unfortunately details are seldom given on the exact cause of the flooding, whether one or several levels or an entire mine were subject to flooding. A tabulation of earthquake effects on tunnels and mines given by McClure (1982) provides comments such as 'mine filled with water', 'mine was flooded', 'existing fractures were opened wider causing increase in water influx and almost flooding mine'. Two of these cases were in California, one was in Chile.

Stevens (1977) suggested that in such cases the earthquakes may have resulted in renewed movement along existing fractures, or that fracturing resulted from the earthquake and provided new avenues for water inflow into the mines.

A recent earthquake in Idaho (2 November 1983) registering 6.9 on the Richter scale caused damage to hundreds of buildings and two fatalities. It also caused a 250% increase in water flow into the 1100 ft deep Clayton silver mine. The mine is located 25 miles west of the epicentre. Flow increased immediately from 1000 gal/min to 2500 gal/min but declined over a six-month period to about 1500 gal/min (Rovetto, 1984).

Flow rates and pressures reportedly increased in numerous locations in the 800 ft and 1100 ft levels, while the 500 ft level produced water for the first time in several years. Major jointing in the local quartzite and dolomite strikes approximately north-south and dips at about 60°. Inflowing water remained clear following the earthquake.

This case is an example of joint conductivity enhancement, rather than fault displacement effects. Furthermore, dynamic stress cycling that occurs only perpendicularly to the joints is unlikely to cause significant increases or decreases in aperture and conductivity if the joint is already under significant levels of effective normal stress. The essentially permanent change in aperture must have been caused by shear-induced dilation across non-planar joint surfaces. Reversed shear and contraction on subsequent cycles of shaking will be inhibited if a significant level of differential stress already exists. The subsequently reduced flows observed in the Clayton silver mine are

probably a function of local drawdown of the groundwater table due to the increased permeability of the rock mass.

Locations having high ratios of principal stress in combination with obliquely dipping persistent jointing will be least able to resist seismic loading due to the likelihood of high shear stress components. A high virgin level of shear stress, perhaps locally accentuated by excavation, would provide the unwanted driving force for progressive, irreversible accumulation of shear displacement during seismic shaking.

As regards rock reinforcement strategies, it is interesting to observe from Figs 16 and 17 that, if shear displacements are controlled, changes in permeability can be reduced to a minimum. For example, slip magnitudes of only 1 mm will mobilize the majority of available shear strength but will not be sufficient to cause marked dilation or changes in conductivity, i.e. a rock reinforcement system that is successful in limiting individual joint displacements to the range 0–1 mm will optimize stability and minimize conductivity changes. A flexible lining such as mesh or fibre-reinforced shotcrete might also tolerate such displacements without cracking. Increased leakage or inflow problems would probably not develop at these levels of shear displacement.

#### STRESS TRANSFORMATION WITH DILATION

When analysing the stability of rock masses it is frequently necessary to transform principal biaxial stress components  $\sigma_1$  and  $\sigma_2$  into their shear and normal stress components  $\tau$  and  $\sigma_n$ . These components are assumed to act across specific joint planes inclined at an angle  $\beta$  to the major principal stress. The classical transformation equations given below are based on the assumptions that the medium is isotropic, the joint planes are imaginary and that they do not slip. At least two of these assumptions are usually violated. In the classical theory

$$\sigma_n = \frac{1}{2}(\sigma_1 + \sigma_2) - \frac{1}{2}(\sigma_1 - \sigma_2) \cos(2\beta) \quad (6)$$

$$\tau = \frac{1}{2}(\sigma_1 - \sigma_2) \sin(2\beta) \quad (7)$$

Besides the violation of assumptions, there is a further very important factor which is not accounted for in equations (6) and (7). As shearing begins along a joint the roughness (if present) is gradually mobilized and results in dilation. This dilation must, by definition, occur out of the plane of the joint. The end result is non-coaxial stress and strain.

It would appear to be simple to correct equations (6) and (7) for this dilation component. However, as indicated in equation (4), the dilation angle mobilized at any instant is a stress- and

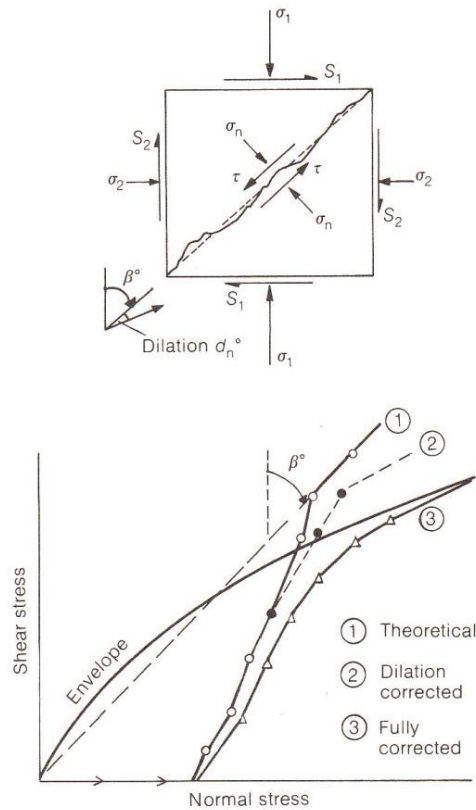


Fig. 18. Corrections for out-of-plane dilation and boundary friction effects explain difficulty in shearing joints under biaxial loading

displacement-dependent variable. It also varies with block size owing to the scale effects on both JRC and JCS.

As reported by Bakhtar & Barton (1984), the failure to account for dilation in the stress transformation can have a marked effect on analysis. Fig. 18 shows a schematic diagram of large-scale biaxial shear tests that were attempted on carefully fractured blocks of rock measuring almost 1 m<sup>3</sup> in volume. The samples were loaded by flatjacks through sheets of polytetrafluoroethylene (PTFE—Teflon). An average friction angle of 10° was measured for the flatjack-PTFE interfaces.

The testing sequence followed in most of the tests was first to load the fractures normally by equal increases in  $\sigma_1$  and  $\sigma_2$ . When the required level of normal stress had been reached,  $\sigma_1$  was increased and  $\sigma_2$  was reduced in an attempt to reach the peak shear strength envelope. The latter was estimated from full-scale tilt tests as illustrated in Fig. 3(a). In every case it was possible to drive the theoretical stress path (Fig. 18, path 1) well above the strength envelope. In several cases shear failure was not achieved until normal stress levels almost twice as high as expected.

It was eventually realized that two corrections were needed to modify the theoretical stress path. A basic error was the initial failure to account for the interface friction components  $S_1$  and  $S_2$ . However, when this had been done, the stress path still climbed above the peak strength envelope without failure.

The second and more fundamental correction was the inclusion of the mobilized dilation angle in equations (6) and (7). The following versions of these equations were found to provide an improved fit to experimental data

$$\sigma_n = \frac{1}{2}(\sigma_1 + \sigma_2) - \frac{1}{2}(\sigma_1 - \sigma_2) \cos [2(\beta + d_{n\text{mob}})] \quad (8)$$

$$\tau = \frac{1}{2}(\sigma_1 - \sigma_2) \sin [2(\beta + d_{n\text{mob}})] \quad (9)$$

As seen in Fig. 18, the fully corrected load path 3 lies beneath the strength envelope and explains the high levels of stress that were needed to reach shear failure. On two occasions the principal stress  $\sigma_1$  was raised to 35 MPa without shear failure, even when  $\sigma_2$  was zero. Higher pressure could not be reached owing to compression failure of the samples which caused the flatjacks to burst explosively.

The apparent failure to include dilation in stress transformations has important consequences in rock mechanics. It is doubtful that stability analyses currently performed in plane strain environments give enough credit to the potential strength and stress changes caused by slip of non-planar joints. Numerical analyses using joint elements or discrete element codes may also be simulating conservative behaviour in this respect.

It is of interest to note from equations (8) and (9) that the inclusion of a  $d_{n\text{mob}}$  component will always increase the normal stress component. However, the shear stress component may increase (for  $\beta + d_{n\text{mob}} < 45^\circ$ ) or decrease (for  $\beta + d_{n\text{mob}} > 45^\circ$ ). In the experimental problem illustrated in Fig. 18, the inclusion of the  $d_{n\text{mob}}$  component will theoretically cause the normal stress component to increase and the shear stress component to decrease. Both these factors will have caused increased difficulty in shearing the rough fractures, as experienced.

The need to account for dilation both in the estimation of shear strength and in the estimation of the shear and normal stress components emphasizes the extreme influence of this parameter. The difficulty of overcoming dilation in a plane strain environment will tend to limit eventual shearing to single features, in place of the mass shearing seen in the failure of rock masses with plane, non-dilatant or clay-filled discontinuities.

#### JOINT DEFORMATION AROUND UNDERGROUND OPENINGS

The foregoing discussion concerning dilation is of particular relevance to the displacement fields measured or predicted around underground openings. The confined plane strain environment will accentuate 'dilation hardening' effects and may cause great differences in behaviour between dilatant and non-dilatant jointing. A true test of the proposed dilation correction will be possible when numerical models that simulate jointing are validated in detail against jointed physical models. This step in the validation process must inevitably precede validation against real cases, where the possibilities of measuring real behaviour are usually limited.

Two classes of models which allow jointing to be simulated in a fairly realistic manner are the physical tension fracture models described by Barton & Hansteen (1979) and John & Rautenstrauch (1979) and the numerical distinct element codes, such as UDEC, developed by Cundall (1980). Both are at present limited to two dimensions. The physical models may consist of tens of thousands of discrete blocks, but variation of joint parameters is inherently difficult owing to their fixed mode of formation. UDEC is not limited to particular constitutive joint laws but is in practice limited to a relatively small number of discrete blocks (hundreds rather than thousands) owing to computation time.

Examples of deformation phenomena observed in physical tension fracture models are reproduced in Figs 19 and 20. The joint or fracture pattern is shown at the correct relative scale in the top right-hand side of each deformation vector plot. The vector plots were produced by computerized stereographic analysis of large photographic negatives, which were exposed at several stages of excavation using a fixed, rigid camera position.

Figure 19 demonstrates a particularly interesting faulting phenomenon, in which the highly anisotropic stress and oblique fracturing caused at least 50 mm of (full-scale) shear displacement on one individual fracture. This displacement initiated as top heading 1 was being excavated and was accentuated during subsequent benching. It is significant that only one of the highly dilatant interlocked tension fractures was seriously sheared. It is reasonably certain that non-dilatant jointing would have shown quite different mass deformation due to multiple slippage, and this would have initiated at lower levels of differential stress.

Figure 20 illustrates the deformation vectors measured around six large cavities excavated close to the surface. The three cavities on the left-

hand side of the figure were under equal horizontal and vertical stress, while the three on the right-hand side had much higher horizontal stress. The relative styles of deformation exhibited by the different fracture patterns demonstrate some of the features illustrated in Fig. 4. For example, model 3 is principally undergoing closure in the arch while model 5 is subjected to a greater amount of shear than normal closure. The stability is thereby compromised. The adverse influences of low horizontal stress and horizontal or sub-horizontal fracturing are seen in model 1 and model 5 respectively.

The model cavities depicted in Fig. 20 were deliberately excavated close to the surface. As such they exhibit a variety of deformation modes that may not be evident to the same degree at greater depth, owing to the reduced degree of freedom. It is generally assumed that jointing plays a smaller role in the overall deformation of a rock mass as the depth from the surface increases. It is also generally assumed that the relative influence of jointing is reduced in weaker rocks.

Both these assumptions are probably correct to a degree. However, it is easy to overlook the increasingly marked contrast in strength between joints of zero tensile strength and highly confined intact rock. Instrumentation of a 1600 m deep shaft in quartzite reported by Barton & Bakhtar (1983b) indicated that jointing can cause highly anisotropic behaviour even at this depth. Extensional strains which were relieved by joint opening on one side of the shaft were subsequently readjusted as stress built up in the concrete lining. Rock-liner interaction was evident when a sudden drop in the tangential liner stress was accompanied by a simultaneous reversal of rock deformation at the same location. However, some of the anisotropic behaviour recorded at this shaft can be explained by an anisotropic distribution of horizontal stress.

An interesting question arises when a perfectly circular opening is combined with isotropic stress and weak rock. What then is the influence of jointing, if any? Will jointing have any effect on performance if it is also orientated perpendicular and parallel to these equal principal boundary stresses? Recent parameter studies performed by the Norwegian Geotechnical Institute (Christianson & Hårvik, 1985) using UDEC (Cundall, 1980) indicate that jointing is still mobilized in shear in such situations, even when the rock is restrained by a high modulus reinforced concrete lining.

Figure 21 illustrates the block model utilized in these numerical experiments. The segmental lining is found to flex slightly at the joints, and

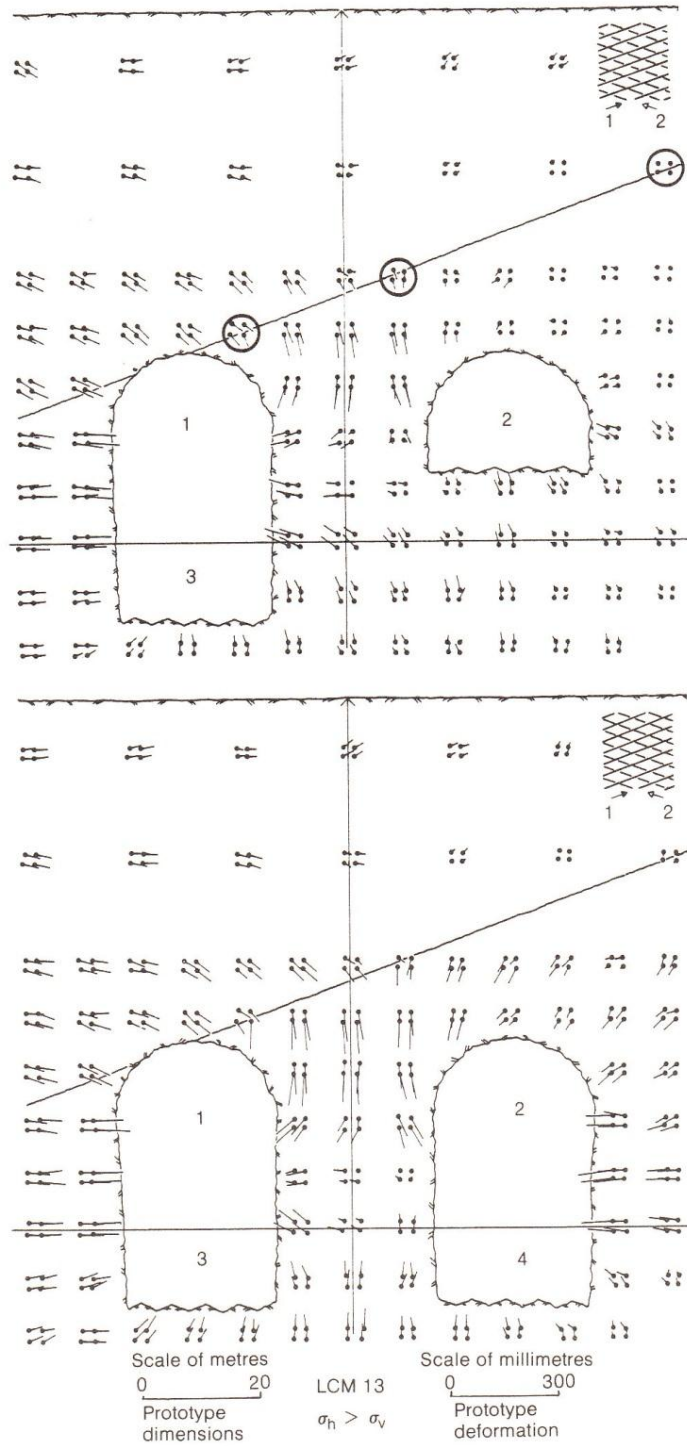


Fig. 19. Example of individual joint shearing in a highly stressed, dilatant physical model of a rock mass (after Barton & Hansteen, 1979)

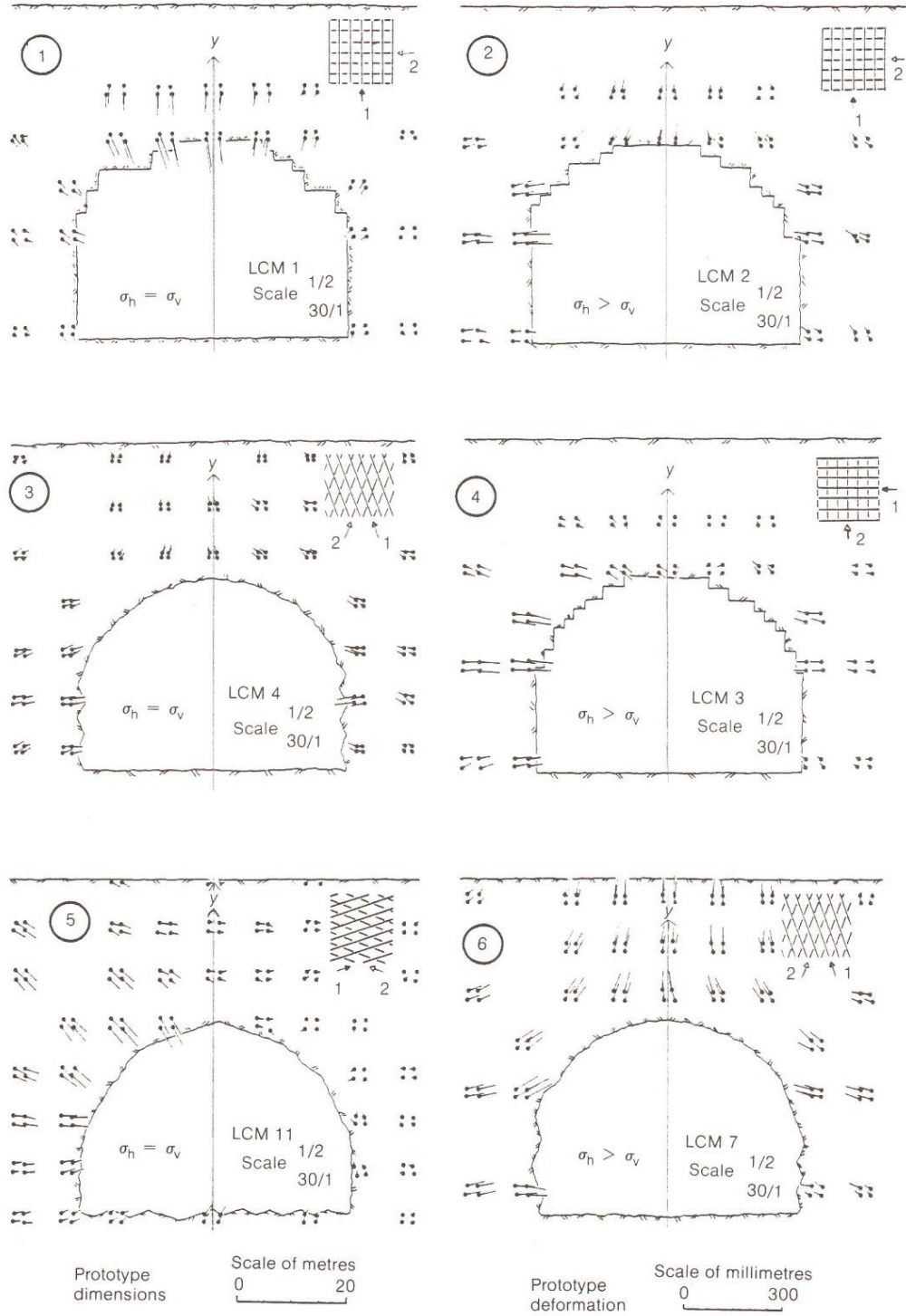


Fig. 20. Influence of joint orientations on deformation modes surrounding near-surface excavations (after Barton & Hansteen, 1979)

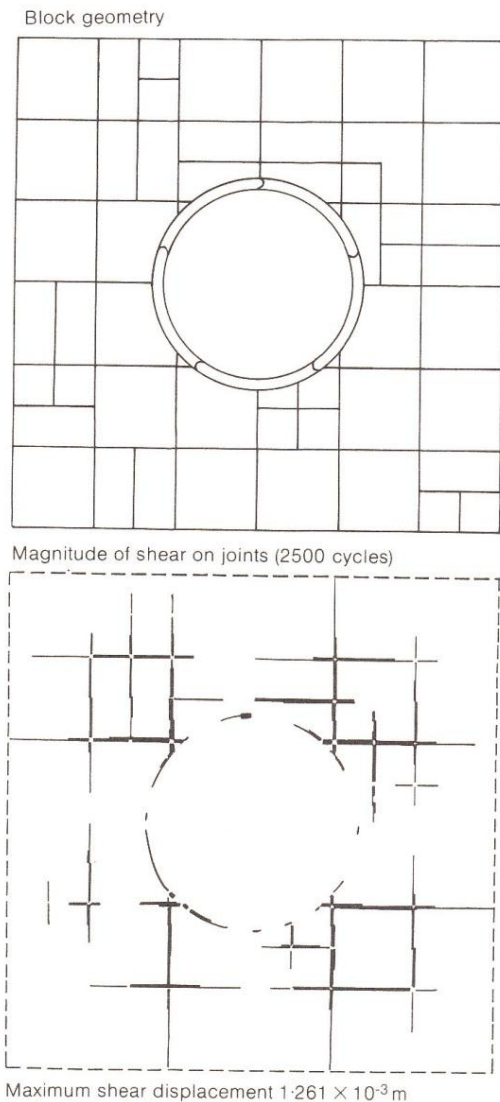


Fig. 21. Joint shearing in an isotropically stressed weak rock with widely spaced jointing using computer code UDEC (after Cundall, 1980) (Christianson & Hårvik, 1985)

shear displacements (proportional to line thickness) are seen to occur along many of the joints. Displacement vectors, which are not shown in the figure, indicate quite anisotropic distributions of deformation, with least deformation between relative positions 6 o'clock and 10 o'clock, where the block size happens to be largest (2 m).

The rock mass modelled in these experiments had the following basic properties

Deformation modulus  $E = 0.3$  GPa

Joint normal stiffness  $k_n = 10$  MPa/mm

Joint shear stiffness  $k_s = 1$  MPa/mm

Principal stresses  $\sigma_1 = \sigma_2 = 10$  MPa

Joint cohesion  $c = 0$

Joint friction  $\phi = 25^\circ$

Joint dilation  $d_n = 1^\circ$

The relatively non-dilatant behaviour assumed for the joints in this weak rock allows slip to occur in many locations. More dilatant joints, which would be realistic for a stronger rock, would have limited slip to fewer locations.

A joint model subroutine incorporating the behaviour shown in Figs 10, 16 and 17 has now been incorporated in UDEC, so that detailed validations can be performed against the physical models shown in Figs 19 and 20. The proposed correction for dilation in the stress transformation equations may prove to be a key aspect in the successful validation of this powerful computer code.

#### CONCLUSIONS

Closure, shear and dilation are three components of joint behaviour that have far reaching consequences for the behaviour of engineering structures in rock masses. Each of the components has a great influence on joint aperture, which can change by orders of magnitude. The cubic relationship between aperture and flow rate is an additional consequence of this extreme sensitivity.

The individual components of joint closure, shear and dilation largely determine the shape and stiffness of load-deformation curves for rock masses. These components also determine the degree of hysteresis and volume expansion effects.

Occurrences of shear displacement and dilation represent the most serious perturbations in a rock mass. They are also the least easily predicted phenomena, being subject to scale effects and causing irreversible behaviour. Unwanted problems in petroleum and geothermal reservoirs can sometimes be attributed to shearing mechanisms induced by fluid pressure changes in anisotropically loaded rock masses.

Dilation accompanying the shear displacement of non-planar rock joints causes changes in the shear and normal stress components and independent changes in the shear strength. These changes can be accounted for by the correct evaluation of the mobilized dilation angle in both the stress transformation equations.

#### ACKNOWLEDGEMENT

The Author is grateful to the following friends and colleagues for direct and indirect contributions to this Paper: Stavros Bandis, Khosrow

Bakhtar, Peter Cundall, Bjørn Kjærnsli, Linda Hårvik and Mark Christianson.

## REFERENCES

- Andersen, K. H. (1970). *Muligheter for store vanntap i trykktunneler på grunn av deformasjoner av slepper i fjellet.* (Possibilities for large leakages in pressure tunnels due to deformation of the discontinuities.) Internal Report F. 382-1, Norwegian Geotechnical Institute.
- Bakhtar, K. & Barton, N. (1984). Large scale static and dynamic friction experiments. *Proc. 25th US Symp. Rock Mech., Evanston*, pp. 457-466.
- Bandis, S., Lumsden, A. C. & Barton, N. (1981). Experimental studies of scale effects on the shear behaviour of rock joints. *Int. J. Rock Mech. Min. Sci. Geomech. Abstr.* **18**, No. 1, 1-21.
- Bandis, S., Lumsden, A. C. & Barton, N. (1983). Fundamentals of rock joint deformation. *Int. J. Rock Mech. Min. Sci. Geomech. Abstr.* **20**, 249-268.
- Barton, N. (1982). *Modelling rock joint behaviour from in situ block tests: implications for nuclear waste repository design.* ONWI-308, Office of Nuclear Waste Isolation, Columbus.
- Barton, N. (1983). Hydraulic fracturing to estimate minimum stress and rock mass stability at a pumped hydro project. *Proc. Workshop Hydraulic Fracturing Stress Measurements, Monterey, 1981*, pp. 61-67.
- Barton, N. (1984). *Rock mass quality and support recommendations for basalt at the candidate repository horizon, based on the Q-system.* Report SD-BWI-ER-012, Revision 1, US Department of Energy Subcontract M46-S88-294292, submitted to Rockwell Hanford Operations, Richland.
- Barton, N. & Bakhtar, K. (1983a). *Rock joint description and modelling for the hydrothermomechanical design of nuclear waste repositories.* Contract Report Parts 1-5, submitted to CANMET, Mining Research Laboratories, Ottawa.
- Barton, N. & Bakhtar, K. (1983b). Instrumentation and analysis of a deep shaft in quartzite. *Proc. 24th US Rock Mech. Symp., Texas A&M University*, pp. 371-384.
- Barton, N. & Bandis, S. (1982). Effects of block size on the shear behaviour of jointed rock. *Proc. 23rd US Symp. Rock Mech., Berkeley*, pp. 739-760.
- Barton, N., Bandis, S. & Bakhtar, K. (1985). Strength, deformation and conductivity coupling of rock joints. *Int. J. Rock Mech. Min. Sci. Geomech. Abstr.* **22**, No. 3, 121-140.
- Barton, N. & Choubey, V. (1977). The shear strength of rock joints in theory and practice. *Rock Mech.* **10**, No. 1-2, 1-54.
- Barton, N. & Hansteen, H. (1979). Very large span openings at shallow depth; deformation magnitudes from jointed models and F.E. analysis. *Proc. 4th Rapid Excavation and Tunneling Conf., Atlanta 2*, 1331-1353.
- Christianson, M. & Hårvik, L. (1985). Private communication.
- Cramer, M. L., Cunningham, J. P. & Kim, K. (1984). Rock mass deformation properties from a large-scale block test. *Bull. Am. Engng Coun.* **XXI**, 47-54.
- Cundall, P. A. (1980). *A generalized distinct element program for modelling jointed rock.* Report PCAR-1-80, Contract DAJA37-79-C-0548, European Research Office, US Army. Peter Cundall Associates.
- Danielsen, S. W. (1971). *Sprekkepermeabilitet.* (Joint permeability.) Thesis, Norwegian Technical University, Trondheim.
- Davison, C. C., Keys, W. S. & Paillet, F. L. (1982). *Use of borehole geophysical logs and hydrologic tests to characterize crystalline rock for nuclear-waste storage.* ONWI-418, Office of Nuclear Waste Isolation, Columbus.
- Hardin, E. L., Barton, N., Lingle, R., Board, M. P. & Voegelé, M. D. A. (1982). *Heated flatjack test series to measure the thermomechanical and transport properties of in situ rock masses.* ONWI-260, Office of Nuclear Waste Isolation, Columbus.
- Heimli, P. (1972). *Vann- og luftlekkasjer gjennom spreker i bergartsstykker.* (Water and air leakage through joints in rock specimens.) *Norw. Rock Mech.*, 137-142.
- John, K. W. & Rautenstrauch, R. (1979). A geo-mechanical model to investigate the effect of dispersed attitude of rough jointing. *Proc. Int. Colloq. Physical Geomechanical Models, Bergamo*, pp. 1-19.
- Kranz, R. L., Frankel, A. D., Engelder, T. & Scholz, C. H. (1979). The permeability of whole and jointed Barre granite. *Int. J. Rock Mech. Min. Sci. Geomech. Abstr.* **16**, 225-234; erratum (1980), **17**, 237-238.
- Lien & Valstad, T. (1971). *Ingeniørgeologisk vurdering av inntakskonus i tilloptunnel.* (Engineering geological assessment of the intake structure for the Bjerka Powerplant headrace tunnel.) NGI Contract Report 70632-1, Norwegian Geotechnical Institute, Oslo.
- Long, P. E. (1983). *Repository horizon identification report.* RHO-BW-ST-28P Draft, US Department of Energy Contract DE-AC06-77RL01030, Rockwell Hanford Operations.
- Makurat, A. (1985). The effect of shear displacement on the permeability of natural rough joints. In *Hydrogeology of rocks of low permeability, Proc. 17th Int. Congr. Hydrogeologists, Tucson*, pp. 99-106.
- McClure, C. R. (1982). Damage to underground structures during earthquakes. *Proc. Workshop Seismic Performance of Underground Facilities, Augusta, 1981*, pp. 75-106.
- Murphy, H., Keppler, H. & Dash, Z. (1983). Does hydraulic fracturing theory work in jointed rock masses? *Trans. A. Meet. Geotherm. Res. Coun.*, 461-465.
- Pine, R. J. & Batchelor, A. S. (1984). Downward migration of shearing in jointed rock during hydraulic injections. *Int. J. Rock Mech. Min. Sci. Geomech. Abstr.* **21**, No. 5, 249-263.
- Pine, R. J. & Cundall, P. A. (1985). Applications of the fluid-rock interaction program (FRIP) to the modelling of hot dry rock geothermal energy systems. *Proc. Int. Symp. Fundamentals of Rock Joints, Bjorkliden*, pp. 293-302.
- Rovetto, R. (1984). Private communication.
- Schrauf, T. W. (1984). *Relationship between the gas conductivity and geometry of a natural fracture.* MSC thesis, Department of Hydrology and Water Resources, University of Arizona.

- Sharp, J. C. (1970). *Fluid flow through fissured media*. PhD thesis, University of London.
- Snow, D. T. (1968). Rock fracture spacings, openings and porosities. *J. Soil Mech. Fdns Div. Am. Soc. Civ. Engrs* **94**, SM1, 73–91.
- Stacey, T. R. (1981). A simple extension strain criterion for fracture of brittle rock. *Int. J. Rock Mech. Min. Sci. Geomech. Abstr.* **18**, No. 6, 469–474.
- Stevens, P. R. (1977). *A review of the effects of earthquakes on underground mines*. Open-File Report 77–313, US Geological Survey.